

---

# Princeton Plasma Physics Laboratory

---

PPPL-

PPPL-



Prepared for the U.S. Department of Energy under Contract DE-AC02-09CH11466.

# Princeton Plasma Physics Laboratory

## Report Disclaimers

---

### Full Legal Disclaimer

This report was prepared as an account of work sponsored by an agency of the United States Government. Neither the United States Government nor any agency thereof, nor any of their employees, nor any of their contractors, subcontractors or their employees, makes any warranty, express or implied, or assumes any legal liability or responsibility for the accuracy, completeness, or any third party's use or the results of such use of any information, apparatus, product, or process disclosed, or represents that its use would not infringe privately owned rights. Reference herein to any specific commercial product, process, or service by trade name, trademark, manufacturer, or otherwise, does not necessarily constitute or imply its endorsement, recommendation, or favoring by the United States Government or any agency thereof or its contractors or subcontractors. The views and opinions of authors expressed herein do not necessarily state or reflect those of the United States Government or any agency thereof.

### Trademark Disclaimer

Reference herein to any specific commercial product, process, or service by trade name, trademark, manufacturer, or otherwise, does not necessarily constitute or imply its endorsement, recommendation, or favoring by the United States Government or any agency thereof or its contractors or subcontractors.

---

## PPPL Report Availability

### Princeton Plasma Physics Laboratory:

<http://www.pppl.gov/techreports.cfm>

### Office of Scientific and Technical Information (OSTI):

<http://www.osti.gov/bridge>

---

### Related Links:

[U.S. Department of Energy](#)

[Office of Scientific and Technical Information](#)

[Fusion Links](#)

# Response of a partial wall to an external perturbation of rotating plasma

C. V. Atanasiu<sup>1,a)</sup> and L. E. Zakharov<sup>2,b)</sup>

<sup>1</sup>Association EURATOM-MEDC, National Institute for Laser, Plasma and Radiation Physics,  
077125 Magurele-Bucharest, Romania

<sup>2</sup>Plasma Physics Laboratory, Princeton University, Princeton, New Jersey 08543, USA

(Received 23 February 2013; accepted 19 August 2013; published online 12 September 2013)

In this paper, we present the response of a 3D thin multiply connected wall to an external kink mode perturbation in axisymmetric tokamak configurations. To calculate the contribution of the plasma perturbed magnetic field in the vacuum region, we have made use of the concept of surface currents [following C. V. Atanasiu, A. H. Boozer, L. E. Zakharov, and A. A. Subbotin, *Phys. Plasmas* **6**, 2781 (1999)]. The wall response is expressed in terms of a stream function of the wall surface currents, which are obtained by solving a diffusion type equation, taking into account the contribution of the wall currents themselves iteratively. The use of stream function makes the approach applicable for both well-studied earlier Resistive Wall Modes and for Wall Touching Kink Modes, which were discovered recently as a key phenomenon in disruptions [L. E. Zakharov, S. A. Galkin, and S. N. Gerasimov, *Phys. Plasmas* **19**, 055703 (2012)]. New analytical expressions, suitable for numerical calculations of toroidal harmonics of the vacuum magnetic fields from the surface currents on axisymmetric shells, are derived. © 2013 AIP Publishing LLC.

[<http://dx.doi.org/10.1063/1.4821124>]

## I. INTRODUCTION

One of the major goals in thermonuclear fusion research is to produce stable high-pressure plasmas, preferably at steady state, for the economic production of fusion energy. High power density implies high  $\beta$  but the maximum magnetic field  $B$  is limited by practical engineering constraints. Ideal magnetohydrodynamic (MHD) instabilities impose hard limits on the achievable  $\beta$ . In tokamaks, if internal instabilities are avoided by a suitable choice of the plasma current profile, the  $\beta$  limit comes about by the onset of Free Boundary Kink Modes (FBKM). They cause a deformation of the plasma boundary, grow on the Alfvénic timescale of the order of  $10^{-6}$ s and can terminate the plasma discharge abruptly.

In the presence of a resistive wall, for non-rotating plasmas and in the absence of active feedback, the stability limit is being virtually the same as in the case without wall. However, the modes grow much more slowly, namely, on the resistive timescale of the wall, which is typically of the order of  $10^{-2}$ s. These decelerated FBKMs are denoted Resistive Wall Modes (RWMs). Therefore, in the presence of a resistive wall, the active feedback stabilization of RWMs by means of magnetic field sensors and a system of additional correction coils becomes technologically feasible.

Stabilization of RWM is one of the key topics addressing prevention of disruptions in tokamaks. There are a vast number of papers investigating the physics of Resistive Wall Modes (see, e.g., Refs. 1–20). In Ref. 1, the authors found that on the time scale over which eddy currents in the wall decay resistively, the magnetic perturbations of external modes penetrate the wall, and the stabilization is lost. In

Ref. 2, the assumption has been made that the eddy currents have negligible radial components, so that the current pattern in the wall is essentially two dimensional—a reasonable assumption in the thin wall limit.

The resistive wall is represented in terms of a set of independent resistors with given “surface resistances”<sup>3,4</sup> with the numerical solution accomplished by coupling the DCON code<sup>6</sup> with the VACUUM code<sup>7</sup> for a tokamak with an arbitrary cross-sectional shape.

In Ref. 16, the magnetic coupling of the toroidal plasma with the resistive wall and other sources of the field asymmetry is formulated. A general formulation for determining the ideal magnetohydrodynamic stability of an axisymmetric toroidal magnetic configuration, including the effects of an arbitrary equilibrium flow velocity and a resistive wall, is presented in Ref. 17.

The effects of 3-D electromagnetic structures on RWM stability of reversed field pinches<sup>18</sup> and a model-based dynamic RWM identification and feedback control in the DIII-D,<sup>19</sup> both using existing numerical codes, have been investigated. Finally, a comprehensive review of the present status of the conceptual foundations and experimental results on the stabilization of the external kink and the resistive wall mode are given in Ref. 20.

The wall response is an important ingredient of realistic modeling of the RMW physics, which is now covered by a variety of numerical codes developed over decades of existence of the topic. In contrast to this, this paper is focused on a new topic, related to disruptions, which emerged when the current sharing effect was discovered in 1996 during a large vertical disruption event on JET, which generated a  $m/n = 1/1$  kink mode ( $m, n$  are its toroidal and poloidal wave numbers), a large sideways force on the vacuum vessel, and the current exchange between plasma and the wall.<sup>21,22</sup> The initially adopted explanation of the current sharing by

<sup>a)</sup>Electronic mail: [cva@ipp.mpg.de](mailto:cva@ipp.mpg.de)

<sup>b)</sup>Electronic mail: [zakharov@pppl.gov](mailto:zakharov@pppl.gov)

so-called halo currents was rejected in Ref. 23 as contradicting all vertical disruption cases on JET in the sight of the effect. Instead, a basic model for the Wall Touching Kink Mode (WTKM) was proposed as consistent with both MHD theory and JET experiments.<sup>24</sup>

This new type of MHD mode is a key element of disruption physics, whose importance became evident regarding the ITER project. As explained in Ref. 24, the new simulation tools, allowing explicit plasma flow into the wall, should be developed in addressing the physics of WTKM. It was found that not only the plasma numerical model in the existing codes has an important deficiency (i.e., inappropriate for the plasma boundary conditions<sup>24</sup>), but even the wall simulations need special numerical schemes. They should be consistent with the spotwise plasma contact with the wall structure and the current sharing between the plasma and the wall.

The present paper was motivated by the fact that most of wall models developed for RWM are not applicable for WTKM. Thus, DCON and VACUUM codes<sup>6,7</sup> are an example of the use of scalar potential representation for the vacuum field. First, it is suitable only for closed toroidal shells without holes, second, WTKM needs the explicit use of electric currents in the wall to describe both Hiro and eddy currents.<sup>24</sup> Several other codes, like, such as the MARS-F code<sup>8</sup> and the KINX code<sup>9</sup> rely on axisymmetric walls. At the same time, 3-D wall structure is essential for the physics of WTKM. VALEN code,<sup>12</sup> one of the first codes which models the 3-D structure of the wall, uses wire mesh representation of currents in the wall, which is singular. Being suitable for RWM, it is not applicable for WTKM, which requires reliable magnetic field and current calculations at the wall surface. The CARMA combination of MARS-F/CARIDDI codes<sup>10</sup> can address realistic stabilization of the slow dynamics of the feedback stabilized RWM. At the same time, the volumetric finite elements (FEs) used for wall representation are inconsistent with the near surface concentrated distribution of the Hiro and eddy currents during the fast stage of disruption. In this regard, the thin wall representation seems to be more appropriate.

The primary interest of the present paper is to simulate the response of a partial wall to magnetic perturbations, as a first step to the complete modeling of the plasma-wall contact in disruptions. Essentially, only one wall model, used for RWM and developed by Merkel (stability code STARWALL and the feedback optimization code OPTIM<sup>13-15</sup>), can be used for WTKM as well. It uses a triangle representation of a conducting thin wall. The same model was developed independently in PPPL by one of the authors (L.Z., Cbsh1 code<sup>24</sup>) but is in the state of calibration against existing experiments.

Here, we present an alternative approach, which is not as universal as triangle-based model, but can be considered as complementary to them due to its very high speed of simulations. In accordance with expected localized area of the plasma-wall contact and of its potential inhomogeneity, as a test of the method, a partial wall surface (5 rad long in the toroidal and 1 rad wide in poloidal directions) is considered. The cases with the holes in the partial wall are included.

Note that the frequently used simplified gradient form of the magnetic field in the vacuum region is not appropriate for the WTKM physics, which exchanges currents between the plasma and the wall as well as simply because of the presence of holes-like spots in the contact area. Instead, the explicit currents in the wall have to be simulated.

An approximate method for the determination of eddy currents in weakly magnetic thin plates and shells whose field is small by comparison with the external exciting magnetic field has been given in Ref. 25. This approach has been used by us to organize the iteration process for self-consistent simulations including the magnetic field from eddy currents.

Other contributions connected directly to the investigation of eddy currents in thin walls are given in Ref. 26 (where the Galerkin method is applied to the integral formulation in terms of current density so as to consider only two scalar functions as unknowns instead of four—the current density vector and the electrical scalar potential),<sup>27</sup> (a mathematical investigation of the validity of the approximation of the Maxwell equations by the eddy currents model),<sup>28</sup> (a numerical method to analyzing transient eddy currents on thin conductors with arbitrary connections and shapes by using the finite element method),<sup>29</sup> (the transient nonlinear 3-D eddy current problem with differential and integral methods),<sup>30</sup> (the approximation of eddy currents in 3D structures with toroidal symmetry),<sup>31</sup> (an FE modelling approach for the calculation of transient eddy currents in thin conductive complex layers),<sup>32,33</sup> and (a Green function method was developed to evaluate the currents induced during startup in the vacuum vessel of ETE (Experimento Tokamak Esférico)). A convenient coordinate system describing the neighborhood of a toroidal thin shell has been reported in Ref. 34 in order to take Halo currents into account.

In this paper, we will present a method to calculate the response of a thin 3D multiply connected thin wall to an External Kink Mode (EKM), based on our first results.<sup>38,39</sup> The paper is organized as follows. Section II is concerned with the formulation of the model problem. The equations governing the time-space dependence of the eddy currents in thin walls are given. In Sec. III, we defined a convenient coordinate system to calculate the eddy current distribution in a resistive thin wall and fix the boundary conditions to be satisfied by the unknown current stream function. Special attention is given to a very efficient solving method developed by us. The obtained numerical results are presented in Sec. IV. Section V is devoted to the calculation of the vacuum magnetic field due to an EKM plasma perturbation. Our analytical approach to check the numerical results is given in Sec. VI. Finally, in Sec. VII, the results are summarized and an outlook for further investigations is given.

## II. FORMULATION OF THE PROBLEM

Two simplifying assumptions will be made. The first one is to consider the plate width small with respect to the other dimensions, i.e., the surface current case is considered. In other words, the skin time of the eddy currents  $\tau_{skin} \simeq \mu_0 \sigma d^2$ , with  $d$  the wall width, has to be sufficiently small in comparison with

the characteristic variation time of the exciting magnetic field. The second assumption consists in considering the magnetic permeability of the wall as  $\mu = \mu_0$ , the permeability of the vacuum. To calculate the contribution of the plasma perturbed magnetic field in the vacuum region in toroidally symmetric tokamak discharges, we have used the concept of a surface current.<sup>40</sup>

The expression of the normal component of the magnetic field produced by the perturbation of the flux function has been calculated using the methodology developed in Ref. 41. In the thin wall approximation, we will consider a coordinate system  $(u, v)$  attached to the wall surface, where  $u$  and  $v$  are representing the poloidal and toroidal directions, respectively.

In a vacuum gap separating the toroidal plasma from the wall and other current-carrying current elements, the perturbed magnetic field can be expressed as  $\tilde{\mathbf{B}} = \tilde{\mathbf{B}}^{pl} + \tilde{\mathbf{B}}^w + \tilde{\mathbf{B}}^{ext}$ , where each term corresponds to the plasma contribution, to the wall contributions and to the electrical currents flowing outside the wall, respectively.

For the purpose of WTKM, the currents in the conducting shell can be reasonably considered as surface currents, dependent on coordinates  $u, v$  on the surface of the wall. Accordingly, they can be represented by two components

$$\mathbf{i} = \mathbf{J} + \nabla\delta, \quad \mathbf{J} \equiv \nabla I \times \mathbf{n}, \quad (1)$$

where

$$\mathbf{J} = \nabla I \times \mathbf{n}, \quad \nabla \cdot \mathbf{J} = 0 \quad (2)$$

is the divergence-free component of the surface current expressed in the term of the stream function  $I(t, u, v)$  and the external normal  $\mathbf{n}$  to the wall. The curl-free component of the surface current  $\nabla\delta(t, u, v)$  takes into account the current shearing between the plasma and the wall

$$\nabla^2\delta = -j_{\perp}(t, u, v), \quad (\nabla \times \nabla\delta) = 0, \quad (3)$$

where  $j_{\perp}$  is the density of the current coming from/to the plasma and acting as a galvanic source for the surface currents on the wall. It should be determined by the physics of the plasma-wall contact, which is beyond the scope of this paper.

The divergence-free part of the surface current in the thin wall is described by the known diffusion equation<sup>3,4,7,15,16,19,25,38</sup>

$$\nabla^2 I(t, u, v) = d\sigma \frac{\partial B_{\perp}(t, u, v)}{\partial t} \quad (4)$$

for the stream function  $I(t, u, v)$ , with  $B_{\perp}$  the normal to the wall component of the magnetic field,  $d$  the wall thickness, and  $\sigma$  the electrical conductivity of the wall. The explicit form of this equation in a curvilinear coordinate system  $u, v$ , used in simulation is presented in Sec. III.

Solving Eq. (3), with  $\delta(t, u, v)$  as unknown and given right hand side, is linked with the diffusion equation for  $I$  through the contribution to  $B_{\perp}^w$ . Solving this equation does not represent numerical problems but is not discussed in this

paper. The real issue is to develop a realistic model for  $j_{\perp}$ , which would be consistent with plasma interaction with the wall during disruptions.

The plasma perturbations are typically represented as a set of toroidal harmonics with a toroidal wave number  $n$ , each containing many coupled poloidal Fourier harmonics. At the wall surface, the appropriate representation can be written as

$$\begin{aligned} B_{\perp}^{pl}(t, u, v) &= B_{mn}^{pl} \exp[-i(mu - nv)] \exp[\gamma^r t + i\omega t], \\ B_{\perp}^w(t, u, v) &= \bar{B}^w(u, v) \exp[\gamma^r t + i\omega t], \\ I(t, u, v) &= \bar{I}(u, v) \exp[\gamma^r t + i\omega t], \end{aligned} \quad (5)$$

where  $\gamma^r$  is the growth rate of the mode in the plasma reference system,  $\omega$  is the angular frequency,  $i$  is the imaginary unit, and  $u, v$  are some poloidal and toroidal angles on the wall. A single Fourier harmonics  $B_{mn}^{pl}$  in the  $B_{\perp}^{pl}$  will be considered as a driving perturbation. The components  $(\bar{I}, B^{pl}, \bar{B}^w)$  are complex values. The diffusion equations for them becomes

$$\nabla^2 \bar{I} = (\gamma^r + i\omega) d\sigma [B_{mn}^{pl} \exp[-i(mu - nv)] + \bar{B}^w]. \quad (6)$$

### III. CALCULATION OF THE EDDY CURRENT DISTRIBUTION IN A RESISTIVE THIN WALL

#### A. Coordinate system

Let us define a curvilinear coordinate system  $(u, v, w)$  where two of the covariant basis vectors

$$\mathbf{r}_u \equiv \frac{\partial \mathbf{r}}{\partial u}, \quad \mathbf{r}_v \equiv \frac{\partial \mathbf{r}}{\partial v} \quad (7)$$

are tangential to the wall surface

$$\mathbf{r}_u \cdot \mathbf{n} = 0, \quad \mathbf{r}_v \cdot \mathbf{n} = 0, \quad (8)$$

where  $\mathbf{r}$  denotes the vector from an arbitrary origin to a variable point and  $\mathbf{n}$  is the external normal to the wall. The third basis vector  $\mathbf{r}_w$  is normal to the wall surface and determines the  $w$  coordinate and is chosen as

$$\mathbf{r}_w \equiv \frac{\partial \mathbf{r}}{\partial w} \equiv d \frac{\mathbf{r}_u \times \mathbf{r}_v}{D}, \quad D \equiv |\mathbf{r}_u \times \mathbf{r}_v|, \quad (9)$$

$d$  is the wall thickness. At the side wall surfaces  $w=0$  and  $w=1$ . The metric tensor has only four non-vanishing components

$$\begin{aligned} g_{uu} &= \mathbf{r}_u \cdot \mathbf{r}_u, \quad g_{vv} = \mathbf{r}_v \cdot \mathbf{r}_v, \quad g_{ww} = \mathbf{r}_w \cdot \mathbf{r}_w = d^2, \\ g_{uv} &= g_{vu} = \mathbf{r}_u \cdot \mathbf{r}_v, \end{aligned} \quad (10)$$

while

$$g_{uw} = g_{wu} = \mathbf{r}_u \cdot \mathbf{r}_w = 0, \quad g_{vw} = g_{wv} = \mathbf{r}_v \cdot \mathbf{r}_w = 0. \quad (11)$$

The contravariant basis vector perpendicular to the plane  $(\mathbf{r}_u, \mathbf{r}_v)$  is given by

$$\mathbf{r}^w = \mathbf{r}_w \frac{1}{d^2}. \quad (12)$$

## B. Surface current density

The current density  $\mathbf{j}$  [A/m<sup>2</sup>] is coplanar with the wall surface

$$\mathbf{j} \cdot \mathbf{r}^w = 0, \quad (13)$$

and can be expressed with the help of a stream function  $I$

$$\mathbf{j} = \nabla I \times \mathbf{r}^w = \frac{1}{dD} \frac{\partial I}{\partial v} \mathbf{r}_u - \frac{1}{dD} \frac{\partial I}{\partial u} \mathbf{r}_v, \quad (14)$$

and corresponds to the surface current density  $\mathbf{i}$  [A/m].  $D = \sqrt{g_{uu}g_{vv} - g_{uv}^2}$  is the 2D Jacobian at the wall surface

$$\mathbf{i} \equiv d \int_0^1 \mathbf{j} dw = \frac{1}{D} \frac{\partial I}{\partial v} \mathbf{r}_u - \frac{1}{D} \frac{\partial I}{\partial u} \mathbf{r}_v. \quad (15)$$

The covariant representation of  $\mathbf{j}$  is

$$\begin{aligned} (\mathbf{j})_u &= \mathbf{j} \cdot \mathbf{r}_u = \frac{g_{uu}}{dD} \frac{\partial I}{\partial v} - \frac{g_{uv}}{dD} \frac{\partial I}{\partial u}, \\ (\mathbf{j})_v &= \mathbf{j} \cdot \mathbf{r}_v = \frac{g_{uv}}{dD} \frac{\partial I}{\partial v} - \frac{g_{vv}}{dD} \frac{\partial I}{\partial u}, \\ (\mathbf{j})_w &= \mathbf{j} \cdot \mathbf{r}_w = 0. \end{aligned} \quad (16)$$

## C. Ohm's law at the wall surface

With the potentials  $\varphi_E$  and  $\mathbf{A}$ , the electric and the magnetic fields are connected via

$$\mathbf{E} = -\nabla \varphi_E - \frac{\partial \mathbf{A}}{\partial t}, \quad \mathbf{B} = \nabla \times \mathbf{A}. \quad (17)$$

Multiplying Ohm's law

$$-\frac{\partial \mathbf{A}}{\partial t} - \nabla \varphi_E = \frac{\mathbf{j}}{\sigma} \quad (18)$$

by  $(\mathbf{r}^w \cdot \nabla \times)$  gives

$$-\frac{\partial(\mathbf{r}^w \cdot \nabla \times \mathbf{A})}{\partial t} - \mathbf{r}^w \cdot \nabla \times (\nabla \varphi_E) = -\frac{\partial(\mathbf{r}^w \cdot \mathbf{B})}{\partial t} = (\mathbf{r}^w \cdot \nabla \times) \frac{\mathbf{j}}{\sigma}. \quad (19)$$

Knowing that  $(\mathbf{j})_w = 0$  and  $\partial(\mathbf{j})_{u,v}/\partial w = 0$ , the curl of vector  $\mathbf{j}$  is

$$\nabla \times \mathbf{j} = \frac{1}{\sqrt{g}} \left( \frac{\partial(\mathbf{j})_v}{\partial u} - \frac{\partial(\mathbf{j})_u}{\partial v} \right) \mathbf{r}_w, \quad (20)$$

where  $\sqrt{g} = \sqrt{\det|g_{ik}|} = dD$  is the Jacobian. We have

$$\begin{aligned} (\mathbf{r}^w \cdot \nabla \times) \frac{\mathbf{j}}{\sigma} &= \frac{1}{dD} \left\{ \frac{\partial}{\partial u} \left[ \frac{1}{\sigma} \left( \frac{g_{uv}}{dD} \frac{\partial I}{\partial v} - \frac{g_{vv}}{dD} \frac{\partial I}{\partial u} \right) \right] \right. \\ &\quad \left. - \frac{\partial}{\partial v} \left[ \frac{1}{\sigma} \left( \frac{g_{uu}}{dD} \frac{\partial I}{\partial v} - \frac{g_{uv}}{dD} \frac{\partial I}{\partial u} \right) \right] \right\}. \end{aligned} \quad (21)$$

We are interested in the normal to the wall component of the magnetic field. Thus, with

$$\mathbf{n} = \frac{\mathbf{r}^w}{|\mathbf{r}^w|} = \frac{\mathbf{r}^w}{\sqrt{\mathbf{r}_w \cdot \mathbf{r}_w/d^4}} = d\mathbf{r}^w, \quad (22)$$

we have

$$\begin{aligned} \frac{\partial(\mathbf{n} \cdot \mathbf{B})}{\partial t} &= d \frac{\partial(\mathbf{r}^w \cdot \mathbf{B})}{\partial t} = \frac{1}{D} \left\{ \frac{\partial}{\partial u} \left[ \frac{1}{\sigma d} \left( \frac{g_{vv}}{D} \frac{\partial I}{\partial u} - \frac{g_{uv}}{D} \frac{\partial I}{\partial v} \right) \right] \right. \\ &\quad \left. + \frac{\partial}{\partial v} \left[ \frac{1}{\sigma d} \left( \frac{g_{uu}}{D} \frac{\partial I}{\partial v} - \frac{g_{uv}}{D} \frac{\partial I}{\partial u} \right) \right] \right\}. \end{aligned} \quad (23)$$

This is a parabolic partial differential equation which describes the distribution of the stream function  $I(u,v)$  in a given wall domain over time. It is solved iteratively, when the source term  $\partial(\mathbf{n} \cdot \mathbf{B})/\partial t$  is considered as known in space and time at each iteration. Then, the contribution of the wall calculated currents is included to the source in the next iteration.

To determine  $I(u,v)$ , appropriate boundary conditions have to be given.

## D. Determination of the boundary conditions

The stream function  $I(u, v)$  has constant values along the real cuts in the wall and edges of the holes. Thus Eq. (23) can be considered as a special kind of boundary value problem which can be thought of as the stable state of an evolution problem. For a wall without holes, if  $I(u, v)$  is a solution, so is  $I(u,v) + C$ , it is sufficient to fix the stream function  $I$  at an arbitrary constant value (there are no currents perpendicular to the boundary) and the Poisson equation can be solved. For the case with holes, this situation changes and we need to know the differences between the constant potentials at the holes boundaries and the constant potential at the exterior wall boundary.

For a constant electrical conductivity  $\sigma$ , we have

$$\nabla \times \mathbf{J} = -\sigma d \frac{\partial(\mathbf{B}^{pl} + \mathbf{B}^w + \mathbf{B}^{ext})}{\partial t}. \quad (24)$$

By multiplying this relation with the surface element  $ds$  and integrating on the surface  $S_\Gamma$  delimited by the  $\Gamma$  curve on which there exists a line current density  $\mathbf{J}$ , we obtain

$$\begin{aligned} \int_{S_\Gamma} \nabla \times \mathbf{J} \cdot ds &= \oint_\Gamma \mathbf{J} d\mathbf{l} = -\sigma d \frac{\partial}{\partial t} \int_{S_\Gamma} (\mathbf{B}^{pl} + \mathbf{B}^w + \mathbf{B}^{ext}) ds \\ &= -\sigma d \frac{\partial \Phi_{S_\Gamma}}{\partial t}, \end{aligned} \quad (25)$$

with  $d\mathbf{l}$  an infinitesimal vector element of surface  $S_\Gamma$ , bounded by the closed contour  $\Gamma$ ,  $d\vec{\Gamma}$  an infinitesimal vector element of the contour  $\Gamma$ . The surface  $S_\Gamma$ , its boundary  $\Gamma$  and the orientation of the normal  $\mathbf{n}$  are set by the right-hand rule.  $\Phi_{S_\Gamma}$  is the magnetic flux through the  $S_\Gamma$  surface. In other words, the curvilinear integral of the current density is proportional to the time variation of the magnetic flux through the considered surface.

In order to eliminate potential multi values of  $I(u,v)$ , artificial cuts should be made in shells, which can carry a net toroidal or poloidal current. The matching conditions across such cuts can be written as

$$I(u_{+\epsilon}, v) - I(u_{-\epsilon}, v) = \text{const}, \quad I(u, v_{+\epsilon}) - I(u, v_{-\epsilon}) = \text{const}. \quad (26)$$

Applied to each hole surface and artificial cuts, Eq. (25) gives the necessary boundary conditions for parabolic equation Eq. (23).

### E. Fast solution algorithm

In the following, we present a fast numerical algorithm we have found using the property of superposition of inhomogeneous and homogeneous solutions for linear equations, such as (23). The stream function  $I$  can be considered as a linear combination,

$$\begin{aligned} I &= \sum_{n=1}^{n_g} C_n F_n^h + F^{nh} \rightarrow \nabla I \times \mathbf{n}_s \\ &= \sum_{n=1}^{n_g} C_n \nabla F_n^h \times \mathbf{n}_s + \nabla F^{nh} \times \mathbf{n}_s, \end{aligned} \quad (27)$$

of an inhomogeneous solution of  $F_n^{nh}$  with 0-values at the edges of the holes and  $n_g$  homogeneous solutions  $F_n^h$  with 0-values at all edges, except one, where  $F_n^h = 1$ .

The unknown constants  $C_n$ , related to the  $I$  values in the holes, can be determined at every over-relaxation iteration used for solving Eq. (23) from

$$\begin{aligned} \oint_{\Gamma_k} \nabla I \times \mathbf{n}_s d\Gamma_k &= \oint_{\Gamma_k} \sum_{n=1}^{n_g} C_n \nabla F_n^h \times \mathbf{n}_s d\Gamma_k \\ &\quad + \oint_{\Gamma_k} \nabla F^{nh} \times \mathbf{n}_s d\Gamma_k \\ &= -\sigma d \int_{S_{\Gamma_k}} \frac{\partial \mathbf{B}}{\partial t} d\mathbf{S}_{\Gamma_k}, \end{aligned} \quad (28)$$

for  $k = 1 \div n_g$ . With the notation  $P_{k,n} = \oint_{\Gamma_k} \nabla F_n^h \times \mathbf{n}_s d\Gamma_k$ , the following system of equations:

$$\begin{aligned} \sum_{n=1}^{n_g} C_n P_{k,n} &= -\sigma d \int_{S_{\Gamma_k}} \frac{\partial \mathbf{B}}{\partial t} d\mathbf{S}_{\Gamma_k} - \oint_{\Gamma_k} \nabla F^{nh} \times \mathbf{n}_s d\Gamma_k, \\ \text{for } k &= 1, 2, \dots, n_g \end{aligned} \quad (29)$$

was obtained with  $C_n$  the unknown constant stream functions on the hole contours.

Such an superposition process eliminates the necessity of nested iterations and gives a significant gain in the speed of simulations, as is illustrated in Table I.

To solve Eq. (23), two approaches have been considered. One, where  $B^{pl}$  has been considered only as l.h.s. of Eq. (23), while  $B^w$  was taken iteratively as a source term and has been calculated by applying the Biot-Savart law for surface currents. The second approach considers  $B^w$  as a part of the l.h.s. of the equation, expressed in terms of the unknown  $I$  via a mutual inductances matrix. Tested for the case of a growth rate  $\gamma$  corresponding to RWMs, the convergence is obtained in very few iterations.

### IV. NUMERICAL RESULTS

The numerical method was tested using a thin wall structure with elliptical cross-section (major axis  $a = 1$  m,  $b = 2$  m, big radius  $R_0 = 3$  m,  $d = 0.001$  m and  $\sigma = 10^6$  S/m)

TABLE I. Comparative running times between a classical solving method and the superposition one for different number of grid points along  $u$  and  $v$  coordinates.

Solving method	Number of grid points	Running time [s]
Dual iterations	$101 \times 101 (u \times v)$	103
Superposition	$101 \times 101 (u \times v)$	3
Dual iterations	$151 \times 151 (u \times v)$	690
Superposition	$151 \times 151 (u \times v)$	14

corresponding to the aspect ratio  $R/a = 3$  and  $\tau \equiv \tau_{wall} = \mu_0 a d \sigma = 4\pi 10^{-4}$  s. Having in mind our final goal—the calculation of WTKMs, we have considered this wall section to measure 5 rad in the toroidal direction and 1 rad in the poloidal direction. This wall is located at the outer part of the plasma and is symmetric with respect to the plasma middle plane. The perturbed magnetic field generated by the rotating plasma has been considered of the form  $B_{\perp}^{pl} = \exp[\gamma^r t] \sin(mu - nv + \omega t)$ . The methodology to calculate this field from a kink mode is given in detail in Sec. V. Two wall cases have been investigated: without and with holes. For both geometries, constant stream function lines corresponding to two distinct scenarios have been calculated. In the first one, a vanishing growth rate  $\gamma^r$  has been considered for a rotating plasma, while in the second scenario, the influence of a non-rotating plasma but with a non-vanishing growth rate of its perturbed magnetic field has been presented. We have considered different values for the dimensionless parameters  $\omega\tau$  characterizing the plasma rotation. In Fig. 1, constant stream function lines calculated for the case of rotating plasma, with a vanishing growth rate, in the presence of a wall without holes are presented, while the same calculations performed in the presence of a wall with holes are given in Fig. 2. Constant stream function lines obtained for non-rotating plasma and a non-vanishing growth rate, in the presence of a wall with holes are reported in Fig. 3. In addition to the case of a partial wall, we have considered the wall as a complete toroidal shell with two cuts along both directions, toroidal and poloidal. The numerical approach was successful in a wide range of rotation parameters and wall geometries relevant to the WTKM.

Special attention has been paid to the errors introduced by the re-entry corners of the holes. For other wall cross-section geometries, Chebyshev polynomials have been used to determine the metric coefficients.

### V. VACUUM FIELD CALCULATION FROM AN EXTERNAL PERTURBATION OF ROTATING PLASMA

Let us consider a sharp-boundary toroidal plasma separated by a vacuum gap from the wall and other current-carrying elements. A FBKM perturbation, for example, can be expressed as

$$\tilde{\mathbf{B}} = \tilde{\mathbf{B}}^{pl} + \tilde{\mathbf{B}}^w + \tilde{\mathbf{B}}^{ext}, \quad (30)$$

where  $\tilde{\mathbf{B}}^{pl}$  is the contribution from the plasma,  $\tilde{\mathbf{B}}^w$  represents the contribution of the wall, while  $\tilde{\mathbf{B}}^{ext}$  is due to the electrical currents flowing outside the wall. In the following, we will

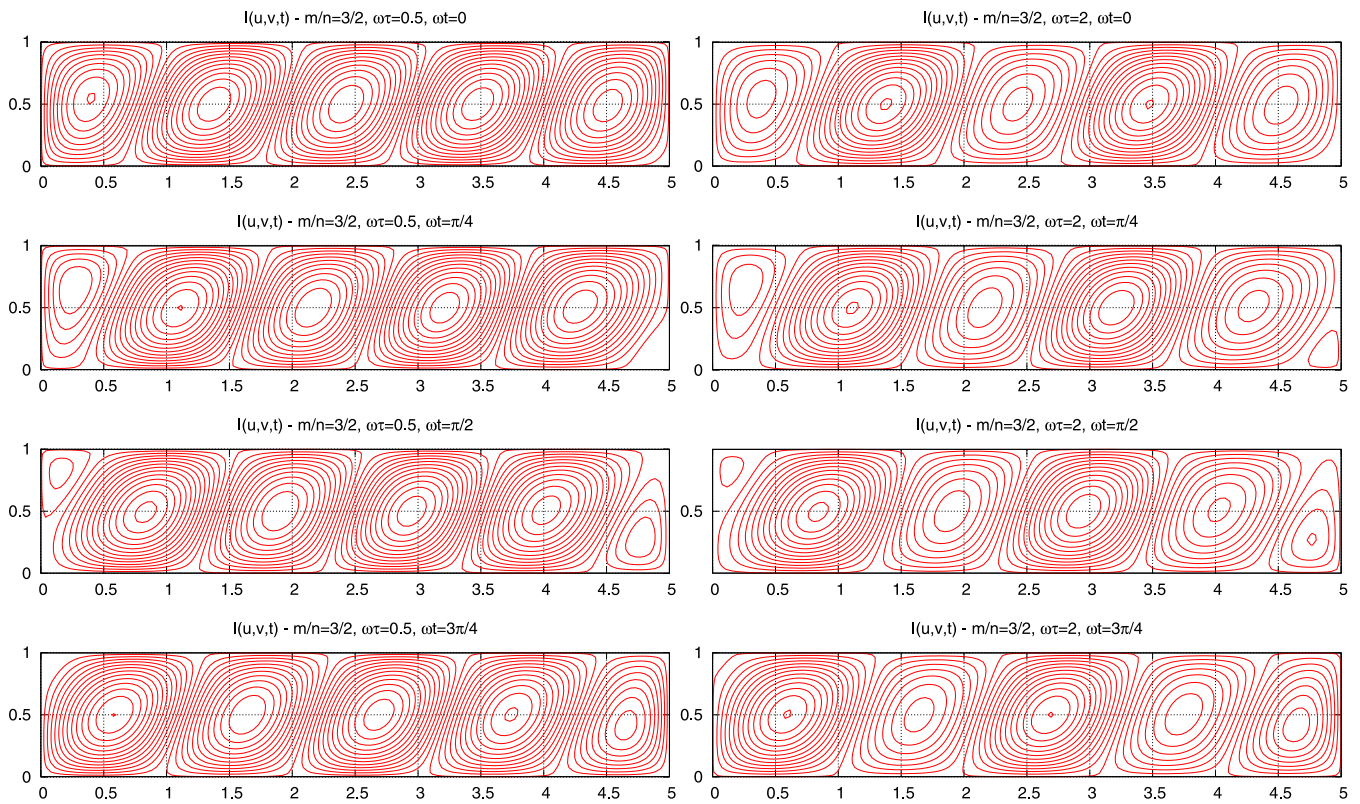


FIG. 1. Constant  $I$  lines (same incremental levels for all figures) in a partial toroidal wall with elliptical cross-section without holes, in the presence of a rotating plasma.  $u \in [0 \div 5 \text{ rad}]$ ,  $v \in [0 \div 1 \text{ rad}]$ . The perturbed magnetic field of the plasma has been considered as  $B_z^{pl} = B_0 \sin(mu - nv + \omega t)$ , with  $\omega\tau = 0.5$  and  $\omega\tau = 2$ . Four phases of wall current distributions are shown, corresponding to the rotating magnetic perturbation.

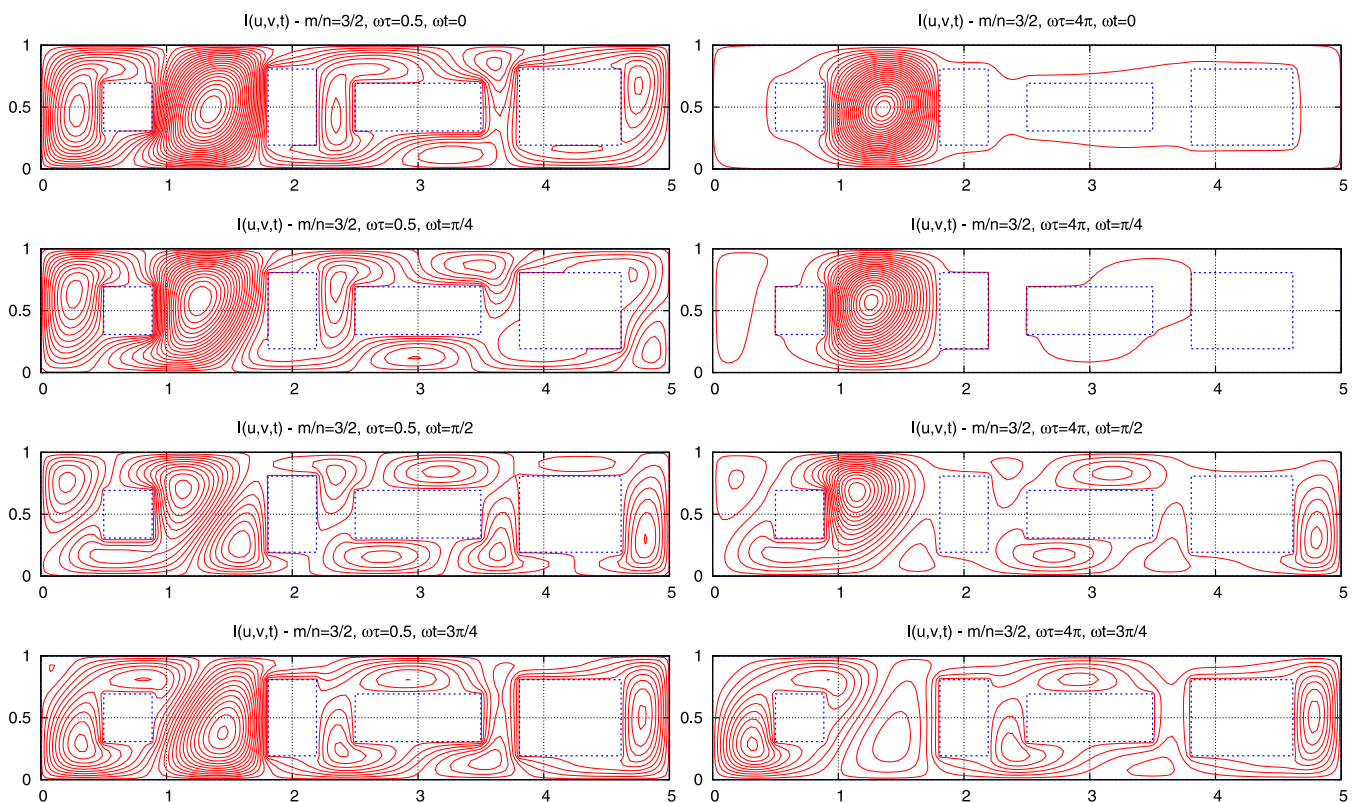


FIG. 2. Constant  $I$  lines for the same partial wall ( $u \in [0 \div 5 \text{ rad}]$ ,  $v \in [0 \div 1 \text{ rad}]$ ) with 4 holes for rotating perturbation  $m/n = 3/2$  and  $\omega\tau = 0.5$  (left side) and  $\omega\tau = 4\pi$ . Four phases  $\omega t = 0, \pi/4, \pi/2, 3\pi/4$  of moving perturbation are shown. The other 4 phases  $\omega t = \pi, 5\pi/4, 3\pi/2, 7\pi/4$  correspond to shown ones in the reversed order.



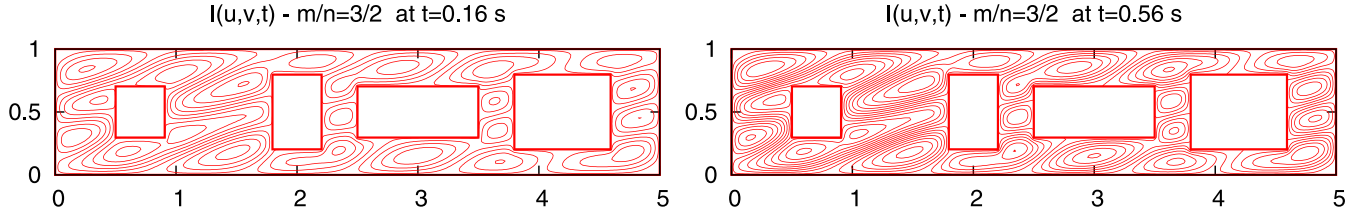


FIG. 3. Constant  $I$  lines in a partial toroidal wall section with elliptical cross-section and holes, for a non-rotating plasma and non-vanishing growth rate, at two different times.  $B^{pl} = B_0 \exp[\gamma' t] \sin(mu - nv)$ .  $u \in [0 \div 5 \text{ rad}]$ ,  $v \in [0 \div 1 \text{ rad}]$ .

calculate the contribution of  $\tilde{\mathbf{B}}^{pl}$  to the normal to the wall magnetic field component.

If somehow we know the flux function perturbation  $\psi$  then in an axisymmetric coordinate system  $(a, l, \varphi)$  attached to the plasma, the tangential and the normal components of the perturbed magnetic field  $\tilde{\mathbf{B}}^{pl}$  are related to the perturbed magnetic flux by the relations<sup>41</sup>

$$\tilde{B}_t = \frac{\nabla a \times \nabla \varphi}{|\nabla a \times \nabla \varphi|} \cdot \tilde{\mathbf{B}} = \frac{\mathbf{e}_l}{|\mathbf{e}_l|} \cdot \tilde{\mathbf{B}} = -\frac{1}{\sqrt{g}} \frac{\partial \psi}{\partial a} + \frac{g_{al}}{\sqrt{g}} \frac{\partial \psi}{\partial l}, \quad (31)$$

and

$$\tilde{B}_\perp = \frac{\nabla a}{|\nabla a|} \cdot \tilde{\mathbf{B}} = \frac{1}{r} \frac{\partial \psi}{\partial l}. \quad (32)$$

$l$  is a contour coordinate along the poloidal direction of the plasma with  $g_{ll} = 1$ ,  $g_{al}$  are the metric coefficients while  $\sqrt{g}$  is the Jacobian.

From potential theory, we know that a continuous surface distribution of simple sources extending over a not necessarily closed Lyapunov surface  $\partial D$ <sup>35</sup> and of density  $\sigma(\mathbf{q})$ , generates a simple-layer potential at  $\mathbf{p}$ , in  $\partial D$

$$\Phi(\mathbf{p}) = \int_{\partial D} \sigma(\mathbf{q}) g(\mathbf{p}, \mathbf{q}) dq, \quad (33)$$

where  $g(\mathbf{p}, \mathbf{q}) = 1/|\mathbf{r}_p - \mathbf{r}_q|$ , with  $\mathbf{r}$  the position vector, is the three-dimensional free space Green's function. Roughly speaking, a Lyapunov surface has a continuously varying tangent plane at each point, but it does not necessarily possess a curvature everywhere (like a separatrix).<sup>35</sup> This potential is continuous everywhere, is differentiable to the second order and satisfies Laplace's equation and is therefore a harmonic function everywhere except at  $\partial D$ . If  $\sigma$  is Hölder continuous at  $\mathbf{p} \in \partial D$ , then the tangential derivatives of  $\Phi$  exist and are continuous at  $\mathbf{p}$ , while the normal derivatives of  $\Phi$  exist and are discontinuous.<sup>36,37</sup>

With  $\tilde{\mathbf{B}} = -\nabla \Phi$  and  $\partial \Phi(\mathbf{p})/\partial n = -\tilde{B}_\perp$ , we can write the basic relation of the magnetic field produced by a general surface charge distribution on a toroidal closed surface  $\partial D$

$$2\pi\sigma(l_p, \varphi_p) + \oint \oint \sigma(l_q, \varphi_q) b_n(l_p, l_q, \varphi_q - \varphi_p) dl_q d\varphi_q = \tilde{B}_\perp(l_p, \varphi_p), \quad (34)$$

with  $l$  a contour coordinate and  $b_n(l_p, l_q, \varphi_q - \varphi_p)$  the normal magnetic field to the unperturbed plasma boundary given by a unit surface charge. In a cylindrical coordinate system  $(r, z, \varphi)$ , the  $(l_p) \equiv (r_p, z_p)$  coordinates represent the field point  $\mathbf{p}$ , while the  $(l_q) \equiv (r_q, z_q)$  coordinates represent the source point  $\mathbf{q}$ . In our attempt to find a surface charge distribution that gives the magnetic field  $\tilde{B}_\perp$ , we have to keep in

mind that as with any magnetic field, the normal components are continuous, while the tangential components present a jump (due to surface currents). In contrast, the tangential derivatives of  $\Phi$  are continuous, while the normal ones jump on  $\partial D$  due to the presence of the surface charge.

We will assume the following "classical" dependencies on  $\varphi$  for fields and charges corresponding to a single mode in a cylindrical coordinate system  $(r, z, \varphi)$ :

$$\tilde{B}_\perp(r, z, \varphi) = \sum_n \tilde{B}_{\perp n}(l) e^{-in\varphi}, \quad \sigma(r, z, \varphi) = \sum_n \sigma_n(l) e^{-in\varphi}. \quad (35)$$

$\tilde{B}_\perp(r, z, \varphi)$  being a real value, the complex values have to fulfill the following conditions:

$$\tilde{B}_{\perp n}(l) = \tilde{B}_{\perp -n}^*(l), \quad \sigma_n(l) = \sigma_{-n}^*(l). \quad (36)$$

The superscript \* indicates complex conjugate values. Note that for axisymmetric toroidal geometry, the individual poloidal harmonics are coupled together, while the toroidal harmonics remain independent.

Equation (34) becomes

$$2\pi\sigma_n(l_p) + \oint \oint \sigma_n(l_q) e^{-in\varphi} b_\perp(l_p, l_q, \varphi) dl_q d\varphi = \tilde{B}_{\perp n}(l_p), \quad (37)$$

where  $\varphi = \varphi_q - \varphi_p$ . Making the notation

$$b_\perp(l_p, l_q) = \oint e^{-in\varphi} b_\perp(l_p, l_q, \varphi) d\varphi, \quad (38)$$

we obtain finally

$$2\pi\sigma_n(l_p) + \oint \sigma_n(l_q) b_\perp(l_p, l_q) dl_q = \tilde{B}_{\perp n}(l_p). \quad (39)$$

The real parts of the normal and tangential field components are given by

$$b_\perp(l_p, l_q) = n_r(l_p) b_{rn}(l_p, l_q) + n_z(l_p) b_{zn}(l_p, l_q), \quad (40)$$

and

$$b_m(l_p, l_q) = t_r(l_p) b_{rm}(l_p, l_q) + t_z(l_p) b_{zm}(l_p, l_q), \quad (41)$$

where  $n_r$  and  $n_z$  are the components of the normal vector,  $t_r = -n_z$  and  $t_z = n_r$  are the components of the tangential vector, while  $b_{rn}$  and  $b_{zn}$  are the  $r$  and  $z$  components of the magnetic field in the application point  $(r_p, z_p)$  given by a unit surface charge located at the plasma boundary. These components are given by the following relations:<sup>40</sup>

$$b_{rn} = \frac{2r_q}{r_p[(r_p + r_q)^2 + (z_p - z_q)^2]^{1/2}[r_p^2 + r_q^2 + (z_p - z_q)^2]} \times \{[r_p^2 - r_q^2 - (z_p - z_q)^2]D_n + [r_p^2 + r_q^2 + (z_p - z_q)^2]C_n\}, \quad (42)$$

$$b_{zn} = \frac{4r_q(z_p - z_q)}{[(r_p + r_q)^2 + (z_p - z_q)^2]^{1/2}[r_p^2 + r_q^2 + (z_p - z_q)^2]} D_n, \quad (43)$$

where

$$C_n = \frac{(1 + \alpha)^{1/2}}{4} \int_0^{2\pi} \frac{\cos n\phi d\phi}{(1 - \alpha \cos \phi)^{1/2}}, \quad (44)$$

$$D_n = \frac{(1 + \alpha)^{1/2}}{4} \int_0^{2\pi} \frac{\cos n\phi d\phi}{(1 - \alpha \cos \phi)^{3/2}}, \quad (45)$$

and

$$\alpha = \frac{2r_p r_q}{r_p^2 + r_q^2 + (z_p - z_q)^2}. \quad (46)$$

Due to the singular nature of the kernels of the second-order Fredholm integral equations, great care has been taken when performing the integrals in the neighborhood of the singularities. We have used both an analytical method and a numerical adaptive method to treat these singularities of the kernels.<sup>40</sup> The method we developed to calculate the periodic integrals  $C_n$  and  $D_n$  is given in Sec. VI.

## VI. ANALYTICAL SOLUTIONS TO CHECK A NUMERICAL APPROACH

We intend to compare the magnetic field produced by surface currents distributed on an axisymmetrical toroidal thin wall, calculated analytically with the magnetic field calculated numerically by a Finite Element Method, recently developed at PPPL (Princeton) to investigate the Hiro currents.<sup>24</sup> In this purpose, we have to calculate the Biot-Savart law for a surface current  $\mathbf{J}$  [A/m]

$$\mathbf{B}(\mathbf{r}) = \frac{\mu_0}{4\pi} \int_{S_\Gamma} \frac{\mathbf{J}(\mathbf{r}') \times (\mathbf{r} - \mathbf{r}')}{|\mathbf{r} - \mathbf{r}'|^3} ds, \quad (47)$$

with  $\mathbf{r}$  the vector radius of the observation point,  $\mathbf{r}'$  the vector radius of the point on the shell, and  $ds$  the surface element of the wall surface  $S_\Gamma$ . The following form of a single toroidal harmonic of the stream function:

$$I(l, \varphi') = \bar{I}(l) \cos n\varphi' \quad (48)$$

specifies the origin of the azimuth  $\varphi'$ . Here,  $l$  is the poloidal length of the shell contour. Accordingly, the unit tangential vector  $\mathbf{t}$  to the wall surface has components

$$\mathbf{t} = t_r \mathbf{e}_{r'} + t_z \mathbf{e}_z, \quad t_r = \frac{dr'(l)}{dl}, \quad t_z = \frac{dz'(l)}{dl}, \quad n_r = -t_z, \quad n_z = t_r, \quad (49)$$

and

$$\begin{aligned} \nabla I &= \frac{\partial I}{\partial l} \mathbf{t} + \frac{1}{r'} \frac{\partial I}{\partial \varphi'} \mathbf{e}_{\varphi'}, \\ \mathbf{J} &\equiv \bar{J}_t(l) \sin n\varphi' \mathbf{t} + \bar{J}_\varphi(l) \cos n\varphi' \mathbf{e}_{\varphi'}, \quad (50) \\ \bar{J}_t(l) &= \frac{n}{r} \bar{I}(l), \quad \bar{J}_\varphi(l) \equiv \frac{d\bar{I}(l)}{dl}. \end{aligned}$$

After straightforward calculations, the expression for practical calculations of magnetic field components of a single toroidal harmonic of the stream function can be represented as

$$\begin{aligned} B_r &= \frac{\mu_0}{4\pi} \cos n\varphi \oint \left( \frac{\alpha}{2rr'} \right)^{3/2} \\ &\quad \times \frac{2}{(1 + \alpha)^{1/2}} \{ \bar{J}_t [t_z r' + t_r(z - z')] (D_{n-1} - D_{n+1}) \\ &\quad + \bar{J}_\varphi (z - z') (D_{n-1}^{3/2} + D_{n+1}) \} r' dl, \quad (51) \end{aligned}$$

$$\begin{aligned} B_\varphi &= \frac{\mu_0}{4\pi} \sin n\varphi \oint \left( \frac{\alpha}{2rr'} \right)^{3/2} \\ &\quad \times \frac{2}{(1 + \alpha)^{1/2}} \{ \bar{J}_t [2t_z r D_n - [t_z r' + t_r(z - z')] (D_{n-1} + D_{n+1})] \\ &\quad - \bar{J}_\varphi (z - z') (D_{n-1} - D_{n+1}) \} r' dl, \quad (52) \end{aligned}$$

$$\begin{aligned} B_z &= \frac{\mu_0}{4\pi} \cos n\varphi \oint \left( \frac{\alpha}{2rr'} \right)^{3/2} \frac{2}{(1 + \alpha)^{1/2}} \{ -\bar{J}_t t_r r (D_{n-1} - D_{n+1}) \\ &\quad + \bar{J}_\varphi [2r' D_n - r(D_{n-1} + D_{n+1})] \} r' dl, \quad (53) \end{aligned}$$

with  $D_n$  given by relations (45)–(46) and with  $\phi = \varphi' - \varphi$ .

In Eqs. (51)–(53), we have to calculate the integrals  $D_n$  for different toroidal wave numbers  $n$ . This represents the most challenging part due to the fact that recurrence relations, similar to those found in Ref. 40, though simple and computationally fast, failed for  $k = [2\alpha/(1 + \alpha)]^{0.5} < 0.4$  and  $n > 4$ . Instead, to overcome this, we have developed a new calculation method of the  $D_n$  integrals by using the associated Legendre functions. An integral representation of the associated Legendre functions is given by<sup>42–44</sup>

$$P_\nu^n(z) = (-1)^n \frac{\nu(\nu-1)\dots(\nu-n+1)}{\pi} \int_0^\pi \frac{\cos(n\phi) d\phi}{[z + \sqrt{z^2 - 1} \cos \phi]^{\nu+1}}. \quad (54)$$

By making the substitution

$$z = \frac{1}{\sqrt{1 - \alpha^2}}, \quad (55)$$

we obtain

$$\begin{aligned} P_\nu^n(z) &= (-1)^n \frac{\nu(\nu-1)\dots(\nu-n+1)}{\pi} (1 - \alpha^2)^{.5(\nu+1)} \\ &\quad \times \int_0^\pi \frac{\cos(n\phi) d\phi}{[1 - \alpha \cos \phi]^{\nu+1}}. \quad (56) \end{aligned}$$

For our special case, the associated Legendre function  $P_\nu^n(z)$  is given by<sup>42-44</sup>

$$P_\nu^n(z) = \frac{\Gamma(\nu + n + 1)(z^2 - 1)^{n/2}}{2^n \Gamma(\nu - n + 1)n!} \times {}_2F_1\left(n - \nu, n + \nu + 1; n + 1, \frac{1 - z}{2}\right), \quad (57)$$

where  ${}_2F_1$  is the hypergeometric function and  $\Gamma$  is the Factorial (Gamma) function. Thus, by using the associated Legendre functions, for  $\nu = -1/2$ , we have obtained the  $C_n$  integral, while for  $\nu = 1/2$ , the  $D_n$  integral has been obtained. For example, the  $D_n$  integrals have been computed exactly up to the ninth digit (double precision) for any  $k$  and for  $n$  up to 20.

Our approach has been applied to the following particular case: a toroidal wall with circular cross-section, with big radius  $R = 4\text{m}$  and small radius  $a = 1\text{m}$  with a surface current distribution of the form  $I = \sin m\theta \cos n\varphi$  ( $\theta$  is a poloidal angle). Two domains where the magnetic field has been calculated have been chosen: one external to the toroidal wall located at  $z \in [-2\text{m} \div 2\text{m}]$ ,  $r \in [0 \div 2\text{m}]$  and the second in the interior of the same wall, located at  $z \in [-0.6\text{m} \div 0.6\text{m}]$ ,  $r \in [3.4\text{m} \div 4.6\text{m}]$ . For all cases we investigated, the toroidal angle of the both domains has been considered intentionally as  $\varphi = 0$  in order to verify how close to the vanishing value of  $B_\varphi$

given by Eq. (52) is the numerically computed  $B_\varphi$  value. The distributions  $B_r(\theta, \varphi)$  and  $B_z(\theta, \varphi)$  in both domains are presented in Figs. 4 and 5.

### VII. CONCLUSIONS

In this paper, a simple fast algorithm for calculation of the response of a thin conducting partial shell to magnetic perturbations is presented. Due to its high speed of calculations, the method is complementary to the more universal approach, based on wall representation by conducting triangles with a uniform current density. The method is consistent with the physics requirements of the Wall Touching Kink Mode and disruption simulations and at the same time is applicable for RWM studies.

The use of curvilinear coordinates, adjusted to the hole geometry was utilized efficiently with high accuracy of computations. While for a cylindrical or elliptical wall cross-section, the metric coefficients could be described analytically, the Chebyshev polynomials interpolation have been tested and used for other wall geometries. A numerical superposition solving method of the stream function equation has been developed and was found to be order of magnitude faster than a straightforward, dual iteration solving method.

Finally, analytical expression have been derived for accurate, high speed calculations of toroidal harmonics of the vacuum magnetic field generated by the surface currents on axisymmetric walls. Unlike earlier used scalar potential

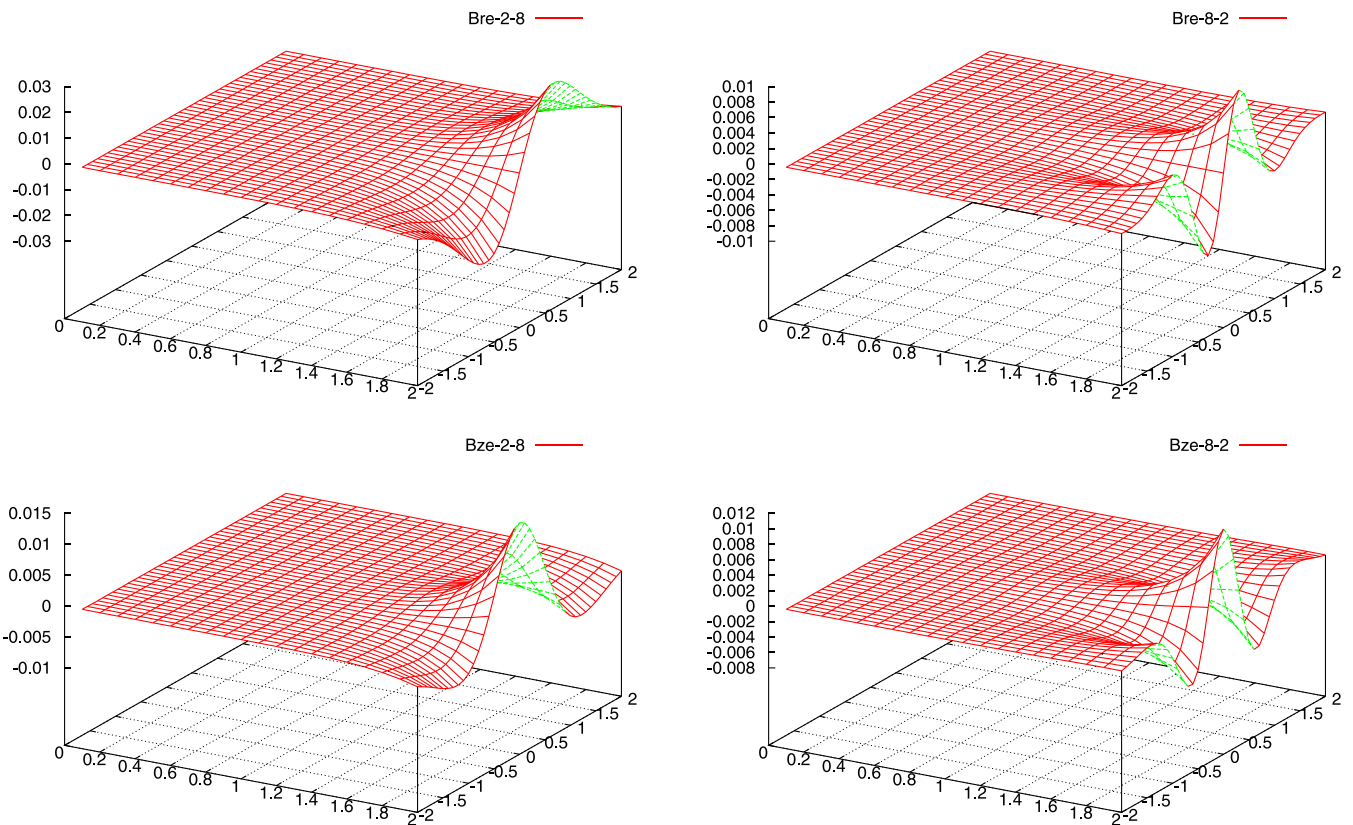


FIG. 4. Distribution of the radial and axial components of the magnetic field  $B_r(r, \varphi, z)$  and  $B_z(r, \varphi, z)$  in an external domain with respect to the wall, given by a surface current distribution of the form  $I = I_0 \sin(m2\pi/Ll)\cos(n\varphi)$  on an axis-symmetric closed tokamak wall.  $L = \int_0^{2\pi} dl$  is the length of the poloidal wall contour. The notation  $Bre - 2 - 8$  on the top of the figures has the following significance:  $Br$  means the radial magnetic field component,  $e$  indicates the external domain where this component has been calculated, 2 represents the poloidal wave number  $m$ , and 8 the toroidal wave number  $n$ .

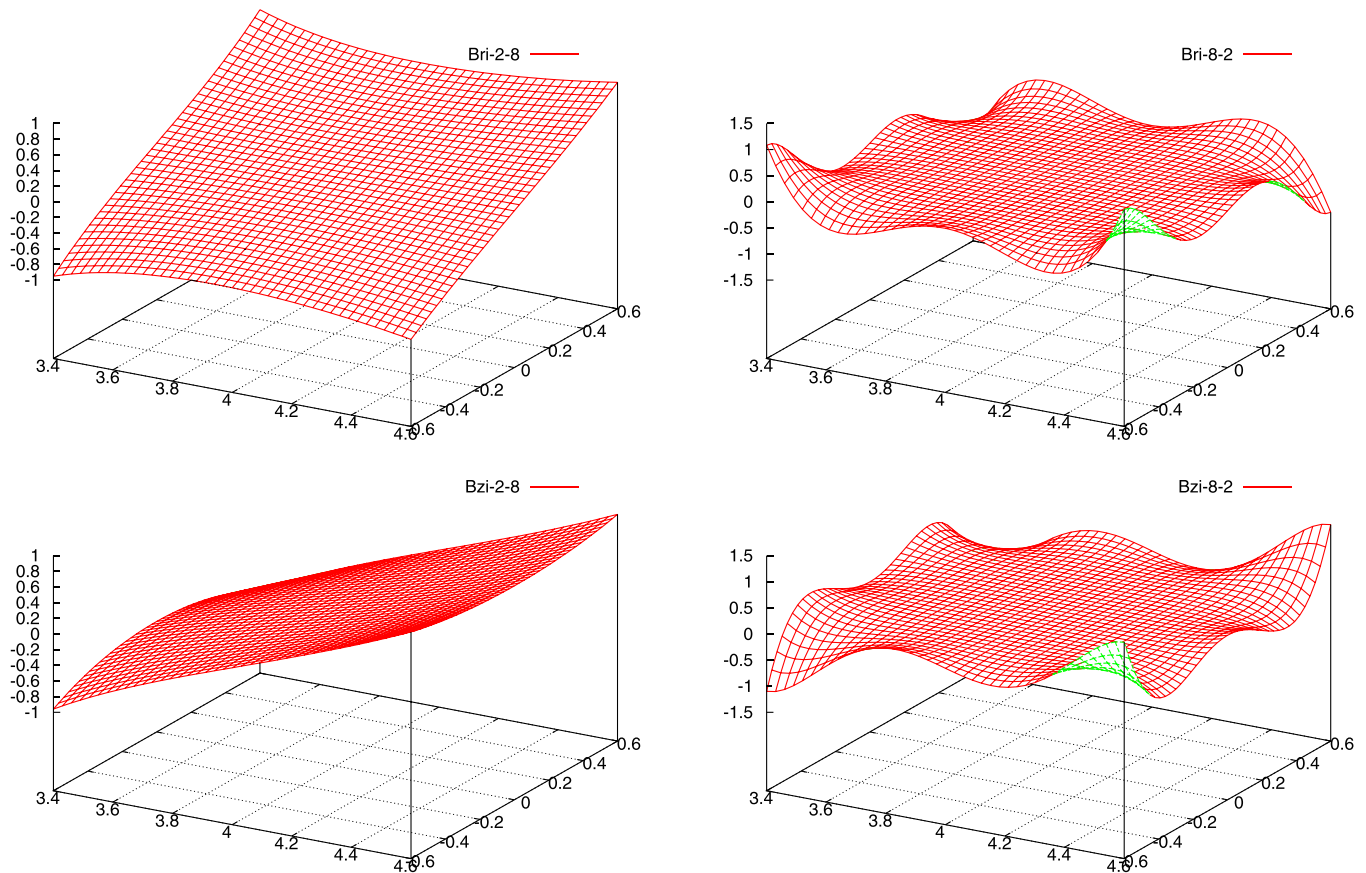


FIG. 5. Distribution of the radial and axial components of the magnetic field  $B_r(r, \varphi, z)$  and  $B_z(r, \varphi, z)$  in an internal domain with respect to the wall, given by a surface current distribution of the form  $I = I_0 \sin(m2\pi/Ll)\cos(n\varphi)$  on an axis-symmetric closed tokamak wall.  $L = \int_0^{2\pi} dl$  is the length of the poloidal wall contour. The notation  $Bzi - 8 - 2$  on the top of the figures has the following significance:  $Bz$  means the axial magnetic field component,  $i$  indicates the internal domain where this component has been calculated, 8 represents the poloidal wave number  $m$ , and 2 the toroidal wave number  $n$ .

expression for vacuum field, the new expressions are suitable for the WTKM and Hiro currents<sup>24</sup> as well.

## ACKNOWLEDGMENTS

Part of this work was conducted during a research stay by C.V.A. to the Max-Planck Institute for Plasmaphysics in Garching, Germany. The hospitality of that Institute is greatly appreciated. This work was partially supported by the Contract BS-1 of the Association EURATOM-MEdC (C.V.A.), and partially by US DoE Contract No. DE-AC02-09-CH11466 (C.V.A. and L.E.Z.).

<sup>1</sup>D. Pfirsch and H. Tasso, *Nucl. Fusion* **11**, 259 (1971).

<sup>2</sup>R. Fitzpatrick, *Phys. Plasmas* **1**, 2931 (1994).

<sup>3</sup>M. S. Chance, M. S. Chu, M. Okabayashi, and A. D. Turnbull, *Nucl. Fusion* **42**, 295 (2002).

<sup>4</sup>M. S. Chu, M. S. Chance, A. H. Glasser, and M. Okabayashi, *Nucl. Fusion* **43**, 441 (2003).

<sup>5</sup>M. S. Chu, A. Bondeson, M. S. Chance, Y. Q. Liu, A. M. Garofalo, A. H. Glasser, G. L. Jackson, R. J. La Haye, L. L. Lao, G. A. Navratil, M. Okabayashi, H. Remierdes, and J. T. Scoville, *Phys. Plasmas* **11**, 2497 (2004).

<sup>6</sup>A. H. Glasser and M. S. Chance, *Bull. Am. Phys. Soc.* **42**, 1848 (1997).

<sup>7</sup>M. S. Chance, *Phys. Plasmas* **4**, 2161 (1997).

<sup>8</sup>Y. Q. Liu, A. Bondeson, C. M. Fransson, B. Lennartson, and C. Bretholtz, *Phys. Plasmas* **7**, 3681 (2000).

<sup>9</sup>L. Degtyarev, A. Martynov, S. Medvedev, F. Troyon, L. Villard, and R. Gruber, *Comput. Phys. Commun.* **103**, 10 (1997).

<sup>10</sup>R. Albanese and G. Ribonacci, *Adv. Imaging Electron Phys.* **102**, 1 (1998).

<sup>11</sup>F. Villone, G. Rubinacci, Y. Q. Liu, and Y. Gribov, *Europhys. Conf. Abstr.* **29C**, P-5.049 (2005).

<sup>12</sup>J. Bialek, A. Boozer, M. E. Mauel, and A. Navratil, *Phys. Plasmas* **8**, 2170 (2001).

<sup>13</sup>P. Merkel and M. Sempf, in *21st IAEA Fusion Energy Conference 2006, Chengdu, China* (International Atomic Energy Agency, Vienna, 2006), Paper No. TH/P3-8, available at <http://www-naweb.iaea.org/naweb/physics/FEC/FEC2006/html/index.htm>.

<sup>14</sup>P. Merkel, C. Nührenberg, and E. Strumberger, *Europhys. Conf. Abstr.* **28G**, P-1.208 (2004).

<sup>15</sup>E. Strumberger, P. Merkel, M. Sempf, and S. Günter, *Phys. Plasmas* **15**, 056110 (2008).

<sup>16</sup>V. D. Pustovitov, *Phys. Plasmas* **15**, 072501 (2008).

<sup>17</sup>L. Guazotto, J. P. Freidberg, and R. Betti, *Phys. Plasmas* **15**, 072503 (2008).

<sup>18</sup>F. Villone, *Phys. Rev. Lett.* **100**, 255005 (2008).

<sup>19</sup>Y. In, J. S. Kim, D. H. Edgell, E. J. Strait, D. A. Humphreys *et al.*, *Phys. Plasmas* **13**, 062512 (2006).

<sup>20</sup>M. S. Chu and M. Okabayashi, *Plasma Phys. Controlled Fusion* **52**, 123001 (2010).

<sup>21</sup>R. Litunovskii, "The observation of phenomena during plasma disruption and the interpretation of the phenomena from the point of view of the toroidal asymmetry of forces," JET Internal Report Contract No. JQ5/11961, 1995.

<sup>22</sup>P. Noll, P. Andrew, M. Buzio, R. Litunovskii, T. Raimondi, V. Riccardo, and M. Verrecchia, in *Proceedings of the 19th Symposium on Fusion Technology, Lisbon*, edited by C. Varandas and F. Serra (Elsevier, Amsterdam, 1996), Vol. 1, p. 751.

<sup>23</sup>L. E. Zakharov, *Phys. Plasmas* **15**, 062507 (2008).

<sup>24</sup>L. E. Zakharov, S. A. Galkin, and S. N. Gerasimov, *Phys. Plasmas* **19**, 055703 (2012).

<sup>25</sup>L. A. Tseitlin, *Sov. Phys. Tech. Phys.* **14**, 1305 (1970) [*Zurnal Techniceskoj Fiziki* **39**, 1733 (1969)].

- <sup>26</sup>R. Albanese, R. Martone, G. Miano, and G. Rubinacci, *IEEE Trans. Magn.* **21**, 2299 (1985).
- <sup>27</sup>H. Ammari, A. Buffa, and J.-C. Nedelec, *SIAM J. Appl. Math.* **60**, 1805 (2000).
- <sup>28</sup>A. Kameari, *J. Comput. Phys.* **42**, 124 (1981).
- <sup>29</sup>R. Albanese, G. Rubinacci, M. Canali, S. Stangherlin, A. Musolino, and M. Raugi, *IEEE Trans. Magn.* **32**, 776 (1996).
- <sup>30</sup>I. Senda, T. Shoji, T. Tsunematsu, T. Nishino, and H. Fujieda, *Nucl. Fusion* **37**, 1129 (1997).
- <sup>31</sup>A. M. Miri, N. A. Riegel, and C. Meinecke, *Int. J. Numer. Model.* **11**, 307 (1998).
- <sup>32</sup>G. O. Ludwig, E. Del Bosco, and J. G. Ferreira, *Nucl. Fusion* **45**, 675 (2005).
- <sup>33</sup>G. O. Ludwig, E. Del Bosco, J. G. Ferreira, and L. A. Berni, *Nucl. Fusion* **46**, S629 (2006).
- <sup>34</sup>A. H. Boozer, *Phys. Plasmas* **19**, 052508 (2012).
- <sup>35</sup>O. D. Kellogg, *Foundations of Potential Theory* (Dover Publications, New York, NY, 1953).
- <sup>36</sup>V. I. Smirnov, *Integral Equations and Partial Differential Equations: A Course of Higher Mathematics* (Pergamon, London, 1964), Vol. IV.
- <sup>37</sup>M. A. Jaswon and G. T. Symm, *Integral Equation Method in Potential Theory and Elastostatics* (Academic Press, London, New York, San Francisco, 1977).
- <sup>38</sup>C. V. Atanasiu, A. Moraru, and L. E. Zakharov, "Influence of a nonuniform resistive wall on the RWM stability in a tokamak," in American Physical Society Plasma 51st Annual Meeting, Atlanta, USA, 2–6 November 2009.
- <sup>39</sup>C. V. Atanasiu, A. Moraru, and L. E. Zakharov, "MHD modeling in diverted tokamak configurations," in 7th ATEE-2011 International Symposium, Bucharest, Romania, 12–14 May 2011.
- <sup>40</sup>C. V. Atanasiu, A. H. Boozer, L. E. Zakharov, and A. A. Subbotin, *Phys. Plasmas* **6**, 2781 (1999).
- <sup>41</sup>C. V. Atanasiu, S. Günter, K. Lackner, and L. E. Zakharov, *Phys. Plasmas* **11**, 5580 (2004).
- <sup>42</sup>A. Erdélyi, *The Bateman Manuscript Project* (McGraw-Hill, New York, 1953), Vol. 1.
- <sup>43</sup>M. Abramovitz and I. A. Stegun, *Handbook of Mathematical Functions* (Dover Publications, Inc., New York, 1994).
- <sup>44</sup>I. S. Gradshteyn and I. M. Ryzhik, *Table of Integrals, Series and Products* (Academic Press, 2007).

The Princeton Plasma Physics Laboratory is operated  
by Princeton University under contract  
with the U.S. Department of Energy.

Information Services  
Princeton Plasma Physics Laboratory  
P.O. Box 451  
Princeton, NJ 08543

Phone: 609-243-2245  
Fax: 609-243-2751  
e-mail: [pppl\\_info@pppl.gov](mailto:pppl_info@pppl.gov)  
Internet Address: <http://www.pppl.gov>